

MECHANICAL AND STRUCTURAL PROPERTIES OF POLY(PHENYLETHYLENE) SYSTEMS: A PRELIMINARY STUDY

ZACHARY FARRUGIA¹ AND JOSEPH N. GRIMA^{1,2}

*¹Department of Chemistry, Faculty of Science
University of Malta, Msida, MSD 2080, Malta*

*²Metamaterials Unit, Faculty of Science
University of Malta, Msida, MSD 2080, Malta*

(received: 8 April 2019; revised: 6 May 2019;
accepted: 10 June 2019; published online: 2 July 2019)

Abstract: The structural and mechanical properties of various types of poly(phenylacetylene) crystalline networked polymers which stack in the third direction in a graphite-like manner have been the subject of extensive research over the past few years. These studies have suggested that depending on the particular manner of substitution of the phenyls, it is possible to achieve some very interesting mechanical properties, which include, in some cases, negative Poisson's ratio (NPR) and/or negative linear compressibility (NLC). The current study investigated how alternatives to these systems can be designed, and specifically tailor-made to exhibit desirable anomalous properties, such as NPR and NLC, through the replacement of the acetylene chains with ethylene chains, so as to produce the poly(phenylethylene) equivalents. Using force field-based simulations, via the use of the polymer consistent force-field (PCFF) it was noted that, to a first approximation, these systems mirror some of the analogous properties exhibited by their poly(phenylacetylene) counterparts. In particular, poly(phenylethylene) systems built from 1234- and 1245-substituted phenyls exhibited negative Poisson's ratios, with the latter also exhibiting negative linear compressibility. This anomalous behaviour, mirrors, to some extent, that exhibited by their poly(phenylacetylene) counterparts, albeit some differences were noted, such as a reduction in the degrees of auxeticity. It was also noted that the poly(phenylethylene) systems modelled here tend to stack in the third direction, in a different manner than their poly(phenylacetylene) analogues, which difference is likely to be the factor for such reduction in auxeticity.

Keywords: auxetics, negative Poisson ratio, organic networked polymers

DOI: <https://doi.org/10.17466/tq2019/23.3/b>

1. Introduction

The field of computational-based materials science has served as a fundamental, and underlying foundation of advancements in several sectors, including industrial, electronics, engineering and others. Systems can either be constructed in such a way to mimic naturally-occurring mechanisms, in order to be better understood, or else constructed through novel designs, which could afford various desirable properties. The use of molecular modelling allows for various theoretical systems to be studied, to various extents, in an attempt to investigate their mechanical, structural, thermal, electronic, and geometric properties of systems on a smaller, more contained manner, which systems could then potentially be scaled up to larger macro-molecular systems.

In this paper, force field-based molecular simulations will be carried out, which allow for structural, geometric and mechanical properties of the required systems to be thoroughly examined. These types of simulations have been chosen in favour of significantly more computationally intensive quantum mechanical-based simulations, like Density Functional Theory or DFT simulations, mainly due to the fact that the latter types of simulations benefit electronic and thermal properties studies more when compared to mechanical, structural and geometric properties studies.

More specifically, this work will be looking into a new class of networked crystalline polymers, poly(phenylethylene) or PE systems, which are meant to mimic the behaviour of known mechanisms which exhibit the anomalous properties of negative Poisson's ratio (NPR) or negative linear compressibility (NLC), as an alternative to the much more well-studied poly(phenylacetylene) or PA systems for the same scope. The PA systems, constructed as networked crystalline polymers, have been predicted, through modelling to be very versatile with properties including in-plane NPR [1–11], out-of-plane NPR [12], NLC [13, 14] and high stiffness [12, 14]. The systems modelled include 135-substituted phenyls, which result in hexagonal networks; 1245-substituted phenyls which result in wine-rack like motifs; and 1234-substituted phenyls, which result in polytriangles-like motifs. The novel PE systems presented and studied here, have a number of desirable features:

1. They can be constructed in a similar manner to their respective PA systems,
2. Have the potential to exhibit the same desirable, anomalous properties, including NPR and NLC,
3. Have the potential to be more tuneable and versatile, which could lead to further research.

It must be said that although there have been a number of theoretical studies on the anomalous poly(phenylethylene) systems, unfortunately, to this date, none of these systems have yet been synthesised. It is thus desirable to assess whether possible alternatives to these systems could be designed, which would retain the predicted anomalous properties without the requirement of having acetylene chains. Such work has so far never been performed.

In an attempt to address this lacuna, this work will aim to investigate the effect on the structure and mechanical properties when acetylene chains are replaced with ethylene chains. In particular, the work will attempt to assess the shapes of poly(phenylethylene) networks vis-à-vis their in-plane and out-of-plane structural properties, with a focus on the manner by which these structures stack when constructed as crystalline systems. An investigation will also be carried out to identify possible stable conformers of these systems, and also to predict the Poisson's ratio and compressibilities, which anomalous properties will be compared to their poly(phenylacetylene) equivalents.

More specifically, in Section 2, the rationale behind the construction of the PA systems chosen for this study, in favour of o systems, will be presented. This is followed by a description of the methodology used to build the structures and the identification of stable minimum energy conformers, through a process of energy minimisation and molecular dynamics (quench molecular dynamics). Similarities and differences between the structures of the novel PE systems, and earlier PA systems will also be identified, as well as the manner by which such systems are expected to stack in 3D.

Section 3 will then attempt to investigate the mechanical properties of the constructed PE systems. This will be performed through calculations of on and off-axis properties, which will include an analysis of Poisson's ratio, Young's modulus, shear modulus and compressibility. Occurrences of NPR and NLC will be discussed in detail.

In Section 4, a conclusion summarising the results previously discussed in the preceding chapters will be presented, along with an account of the strengths and limitations of the current work. Furthermore, advice on any potential further work, especially given the preliminary nature of this work, will be outlined.

2. Simulation of the poly(phenylethylene) systems

As outlined in Section 1, the main objectives of this paper is to simulate a series of poly(phenylethylene) systems as alternatives to the well-known and well-studied poly(phenylacetylene) systems modelled in [2–6, 8, 9, 12, 14], with the scope of assessing how replacing the acetylene chain with its ethylene equivalent can affect the structural and geometric properties, in this section, and the mechanical, and subsequently related properties in the following section.

Poly(phenylacetylene) networks, henceforth referred to as PE networks, are made up of acetylene chains which behave as 'rigid' connectors between phenyl rings, allowing for particular negative Poisson's ratio and negative linear compressibility features to arise. These systems have been the subject of extensive research over the past years demonstrating interesting and novel properties, though their ethylene counterparts have not been so thoroughly analysed. This paper aims to investigate any similarities and dissimilarities between the systems, along with any potential novel characteristics.

2.1. Systems modelled

The systems modelled may be considered as infinitely large 2D networks, shown schematically in Figure 1 and their homologues with longer ethylene chains, having $n \in \{1, 2, 3, 4, 5, 6, 7\}$ double bonds in their ethylene chains. They have been represented as crystalline systems with full periodic boundary conditions being imposed, and no additional symmetry constraints. Parallel layers of these networks were permitted to stack freely as graphite-like crystalline systems allowing for free interaction between layers. Note that, as discussed below, these systems are the analogues of the ones modelled elsewhere [14], having acetylene chains in lieu of the ethylene chains and are meant to mimic a number of well-known structures for which anomalous mechanical and structural behaviour has been attributed.

Depicted in Figure 1(a) to 1(h) are diagrammatic representations of the PE systems modelled, as well as their PA counterparts.

In particular the systems in Figure 1(c) may be described in terms of connected, corner-sharing equilateral triangular units having their sides made from ethylene chains which are connected together via phenyl rings. The 1,2,3,4-substitution pattern of the phenyl rings, as shown in Figure 1(c), permits the internal angle of the triangles to be 60° , as defined by equilateral triangles, provided by the 1,2- and 3,4-substitutions. This also permits two adjacent triangles to be at an angle of 60° to each other. This type of connectivity, involving the use of phenyl rings as the connecting unit, is analogous to that used previously by Grima and Evans [4], in their work on the equivalent systems shown above, where the ethylene chains were replaced by acetylene ones. From a structural perspective, the use of ethylene instead of acetylene, is expected to give the triangles *some* additional degrees of freedom, which was not present in the original poly(phenylacetylene) systems.

Here it must be emphasised that unlike their counterparts constructed from sp^3 -hybridised carbon atoms, where the carbon atoms would have been inter-connected via single bonds which permit *quasi*-free torsional rotation, in this case, recognising that the chains are all made of hyper-conjugated sp^2 -hybridised carbon atoms, an amount of hindrance in rotation around the C=C bonds, due to the nature of the pi bonding, is expected, meaning that the ethylene chain is expected to behave like a (rigid) ‘nano-beam’. Nevertheless, the lack of full rotational symmetry about the length of the chain, when compared to the counterparts made from sp -hybridised atoms, give the present system the possibility to adopt different conformations in space, even as a result of very minute changes in the torsion angles.

From a chemistry perspective, the use of ethylene chains also introduces the possibility of functionalisation of the system since the ethylene chains contain a number of hydrogen atoms which could potentially be replaced with other functional groups. For this work in particular, only the hydrogen substituted systems will be considered, as the main scope of the dissertation is to assess the effect of replacing ethylene chains with the acetylene chains. In accordance with

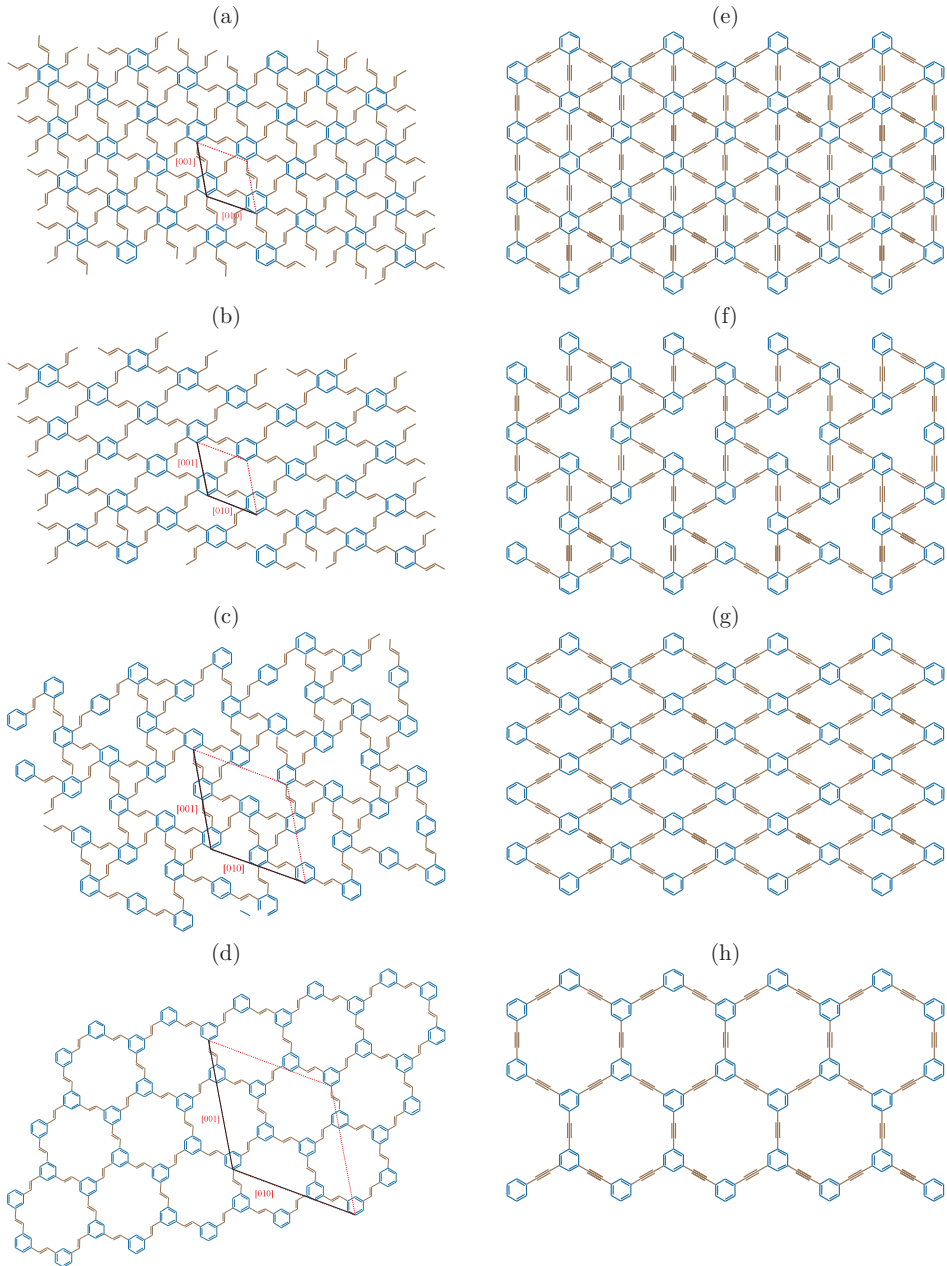


Figure 1. Diagrammatic representation of (a-d) the poly(phenylethylene) systems modelled in this work, and (e-h) the poly(phenylacetylene) systems modelled in [14]

the nomenclature introduced in [15], the poly(phenylethylene) systems will be referred to as PE123456- n , where n represents the number of double bonds within the chains, the letters PE indicate that the constituents of the system are phenyl groups and ethylene groups, while the 1234 indicates the manner of substitution in

the ring. Note that the poly(phenylacetylene) equivalents are termed PA1234-*n*, where the A indicates that the chains are acetylene ones.

Similarly, the structure in Figure 1(b), has the essential geometric features to make it describable as a wine-rack-like unit, with the angle between the ligaments (ethylene chains), being 60° and 120°, values dictated by the 1245-manner of substitution on the connected phenyl rings. Once again, this system can be considered as the analogue of the acetylene wine-rack-like system modelled in [15], which was shown to exhibit negative Poisson’s ratio and negative linear compressibilities, properties which had also been predicted through analytical modelling in [13]. In this case, these poly(phenylethylene) systems will be referred to as PE1245-*n* systems.

Also constructed were systems with 135-alternating substitution, shown in Figure 1(d), which resulted in the formation of honeycomb-like systems, along with the fully substituted 123456-substituted systems which are analogous to the well-known graphyne, graphidyne, *etc.*, systems (see Figure 1(a)). These systems will be referred to as PE135-*n* and PE123456-*n* systems, respectively.

At this point it should be noted that all the PE systems were constructed using a *trans* mode of connection, rather than *cis*. This choice was deliberately made in view of the fact that, from a purely geometric perspective, the *trans* mode of connection, permits the structure to easily adopt planar conformations. In fact, simulations performed on a basic building block of these systems, as shown in Figure 2, showed that whilst a *trans* triangular unit adopts a *quasi*-perfectly planar conformation, its *cis* counterpart tends to minimise to a cup-like conformation which bears some similarity to what one normally observes in calixarenes.

These simulations were performed on the units shown in Figure 2, constructed as isolated single molecules. The energy expression was set up using the Polymer Consistent Force Field (PCFF) [16, 17], as implemented within the Forcite module in Materials Studio 7.0. (Accelrys[®] Inc.) This force-field is a second-generation force-field, which includes valence terms (stretching terms, bending terms, torsion angles and inversion terms), non-bond terms (van der Waals and electrostatic terms), and various cross-terms. In this case, the default settings, including the partial charges¹ used on the atoms, and the method of summation for non-bond terms, where a spline cut-off was used to curtail the non-bond terms, with a cut-off value of 18.5 Å and spline width of 1 Å, were used. The minimiser used was the Smart algorithm which involves successive runs of three algorithms, namely the steepest descent, ABNR, and *quasi*-Newton methods. Minimisation was carried out until the pre-defined, default, ultra-fine convergence criteria for the Geometry Optimisation Task of the Forcite module, were met (maximum energy change of 2×10^{-5} kcal mol⁻¹ between minimisation steps, a maximum force of 1×10^{-3} kcal mol⁻¹ Å⁻¹, and a maximum atom displacement of 1×10^{-5} Å).

1. The default method for assigning charges in PCFF, as implemented in the Forcite Module, is via the bonds-increment method, which is known to result in neutral molecules when the method operates.

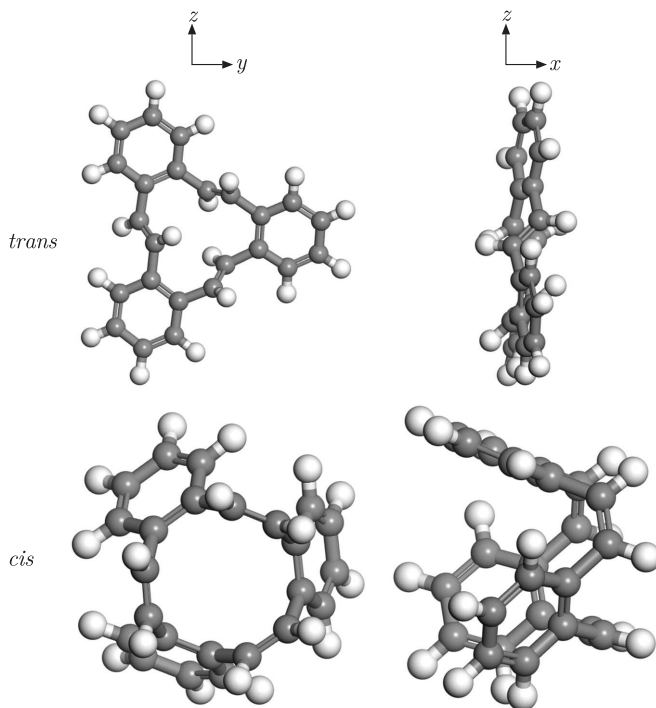


Figure 2. *Trans* vs *cis* configurations of the modelled building blocks of poly(phenylethylene) structures, as seen in the *zy*- and *zx*- directions

Additionally, it was ensured that the charges computed during said simulations were realistic. In this particular case, the charges computed via the PCFF bond-increment method, were compared to the ones obtainable using the charge-equilibration method [18]. Results have shown that in the case of systems where the chains are made from sp^2 -hybridised carbon atoms, there was an agreement in the manner by which the charges were distributed. It was also noted that the systems made from sp -hybridised carbon atoms, had unrealistic charges assigned to the sp -hybridised carbon atoms, when the PCFF method was used, since these were all given a positive charge, which would result in an overall positively charged molecule. In contrast, the charge-equilibration procedure gave a more realistic distribution of charges, which ensured overall neutrality. Given that it is not the scope of this work to model the poly(phenylacetylene) systems, the present work will always make use of the bond-increment method to calculate charges, since this is an appropriate method for the systems.

Furthermore, apart from the difference in shape, it is also interesting to note that the *trans* form has a slightly lower potential energy than the *cis* version, as one may note in Table 1, where the contributions to the potential energies of the system in terms of the force-field component are listed. This table suggests that the slight stabilisation from the non-bonding terms of the *trans* over the *cis* of $1.57 \text{ kcal mol}^{-1}$ is almost negligible compared to the increase in the bonding terms

Table 1. The energy contributions of *cis* and *trans* building blocks modelled

	<i>cis</i>	<i>trans</i>
Total energy (kcal/mol)	49.08	42.97
Contributions to total energy (kcal/mol)		
Valence energy (diag. terms)	31.50	23.57
Bond	3.91	3.79
Angle	5.34	3.24
Torsion	22.11	16.50
Inversion	0.14	0.04
Valence energy (cross terms)	-3.89	-3.63
Stretch-Stretch	0.43	0.41
Stretch-Bend-Stretch	-0.88	-0.79
Stretch-Torsion-Stretch	-1.36	-1.40
Separated-Stretch-Stretch	0.30	0.28
Torsion-Stretch	-8.86	-8.64
Torsion-Bend-Bend	0.07	0.07
Bend-Torsion-Bend	6.41	6.44
Non-bond energy	21.46	23.03
van der Waals	12.27	16.40
Electrostatic	9.19	6.64

(7.93 kcal mol⁻¹), particularly the torsion angle terms. This further confirms the choice of the *trans* conformation over the *cis*.

2.2. Simulations of building blocks

In an attempt to test the hypothesis that structural differences are expected between the systems made from chains of sp²-hybridised carbon atoms, connected via double bonds, (poly(phenylethylene) chains), and their counterparts modelled in earlier work [2, 3, 19, 5, 6, 8, 9, 12, 14], made from chains of sp-hybridised carbon atoms, connected via triple bonds (poly(acetylene) chains), simulations on the building blocks of these systems, namely a triangular unit, a rhombic unit, and a hexagonal unit, were performed using the settings as above on the building blocks of both the PE and PA systems. These simulations were performed using the settings as in Section 2.2, *i.e.* using the PCFF force-field with its default bond-increment method for partial charge calculation², spline summation method for non-bond interactions, and the Smart minimiser as implemented in the

2. Note that, the charges calculated for the PA systems, are not likely to be realistic, as the carbon atoms on the acetylene chains were all given an equal and non-negligible positive charge, making the systems overall positive. In view of this, simulations were also repeated using charges computed by the charge equilibration method, where the findings were not qualitatively different from those shown here.

Forcite module for energy minimisation, which were carried out to the ultra-fine convergence criteria.

Images of the minimum energy structures obtained, are shown below in Figure 3, which clearly illustrates some of the more salient similarities and differences between these two types of systems. In particular, all systems minimised with the required 2D profiles (triangular, rhombic, or hexagonal). However, whilst the PA systems, have all minimised to a form which, to a first approximation, can be considered as perfectly planar structures, the PE systems, minimised to conformations having considerable out-of-plane distortions. This confirms the hypothesis that the PE systems modelled here can be considered as being more flexible/structurally versatile than their PA counterparts but are still ‘rigid’ enough so as to permit their use to construct networks having the required triangular, rhombic and hexagonal geometries.

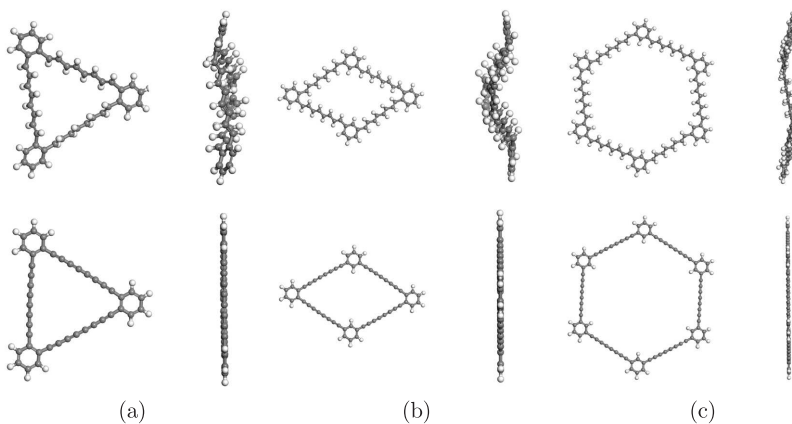


Figure 3. Differences in the geometrically optimised building blocks of (a) PE1234-4 vs PA1234-4, (b) PE1245-4 vs PA1245-4, and (c) PE135-4 vs PA135-4

It may thus be concluded that the PE systems may provide a viable alternative to the PA systems studies so far, and should be further investigated.

2.3. Simulations of crystalline systems

In view of the findings from the previous section, simulations were performed on the PE123456- n , PE1245- n , PE1234- n , PE135- n where $n \in \{1, 2, 3, 4, 5, 6, 7\}$ (a total of $4 \cdot 7 = 28$ systems) using the molecular modelling package Materials Studio running on FUJITSU CELSIUS desktop PC, with an Intel® Core™ i7-8700 CPU, an AMD Radeon Pro WX 3100 GPU and 32 GB of DDR4-RAM, with the scope of investigating their structural and mechanical properties. The procedure used to prepare these model systems involved:

1. Construction of the systems modelled
2. Setting up of the Energy Expression
3. Identification of stable conformations via Energy Minimisation and Quench Molecular Dynamics and their structural analysis

following which the mechanical properties (on-axis and off-axis) were calculated (see Section 3). Perl scripting was used whenever possible to minimize human error and maximise efficiency and all simulations were carried out using the Forcite module.

2.3.1. Construction of systems modelled

The PE systems to be modelled were all represented as crystalline systems where the unit cell of each structure was oriented in space such that the [001] direction lied parallel to the global z -axis, and the [010] direction was aligned in the yz -plane. This results in a construction where the network layers lie parallel to the yz -plane. In analogy to earlier work in [14], the different layers were allowed to stack freely and interact with each other to create a graphite-like system. This free stacking was permitted by letting the [100] cell direction to adopt any magnitude and orientation in space. This type of alignment was used so as to facilitate analysis of the properties and compare them with their equivalent ones, namely PA123456- n , PA1245- n , PA1234- n , PA135- n .

Given that the PE1245- n , PE1234- n , PE135- n systems can be considered as being the non-fully substituted analogues of PE123456- n system, the latter systems were constructed first, from which the others were obtained through deletion of appropriate portions within the network, and hydrogen adjusting. The procedure used exemplified through the PE123456-1 system, *i.e.* the fully substituted network with just one double bond adjacent to the phenyl rings, is described graphically in Figure 4.

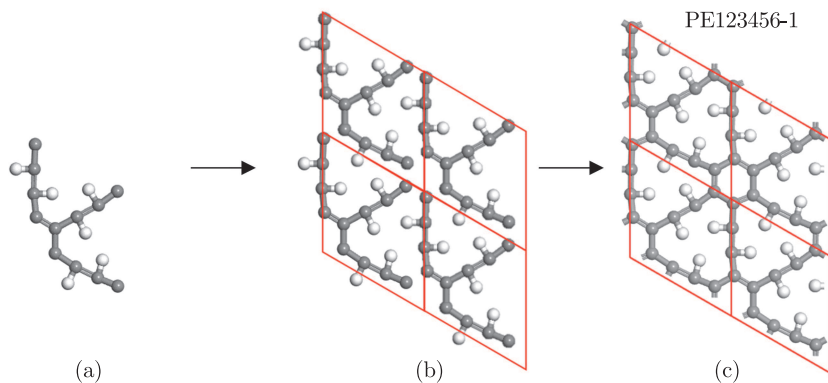


Figure 4. The construction method used, from a basic structure, resulting in PE123456-1

As shown in Figure 4, PE123456-1 was constructed by inputting three but-2-ene chains, and joining them to form half a phenyl ring (see Figure 4(a)). The next step involved the construction of a 2×2 unit cell, with adequate cell parameters (see Figure 4(b)). The four adjacent separate unit cells were then connected, by adding bonds between the phenyl carbons (see Figure 4(c)). It is important to note that the *trans* method of substitution was adopted, in view of what was previously discussed.

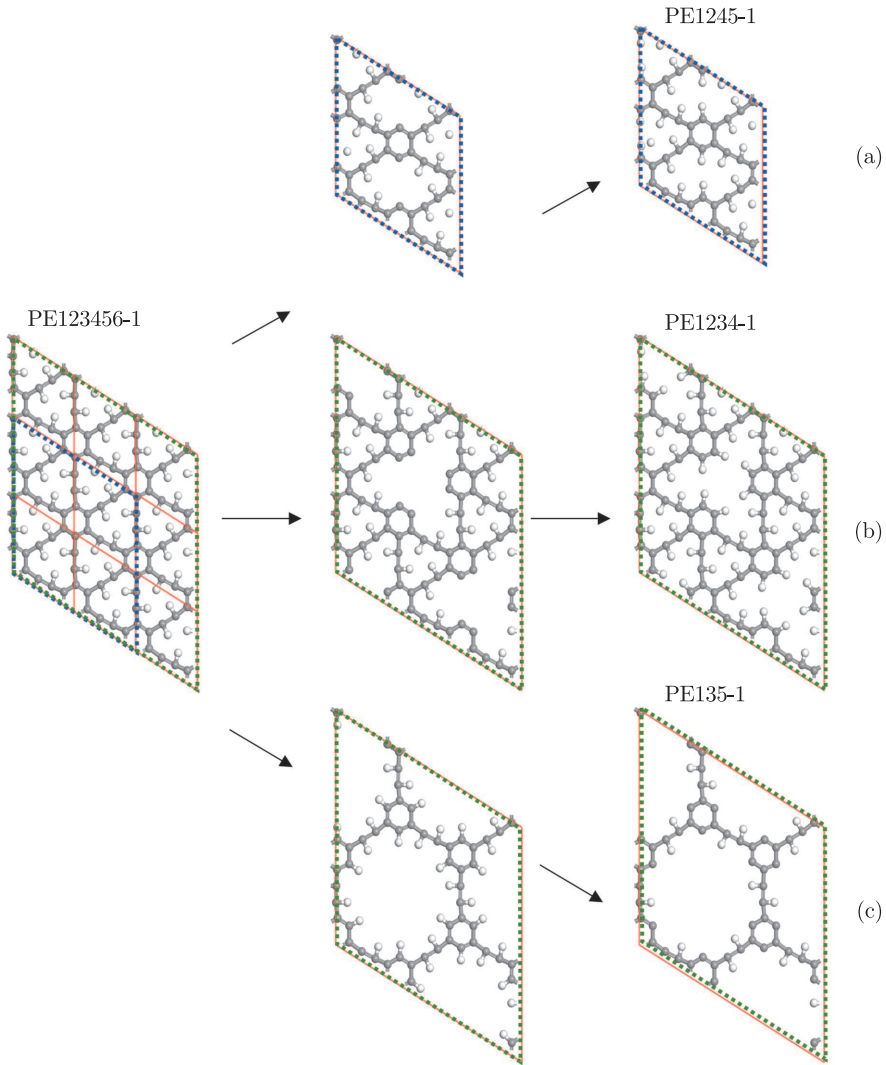


Figure 5. The construction method used, to obtain (a) PE1245-1; (b) PE1234-1; and (c) PE135-1, starting from the PE123456-1 structure previously constructed

As shown in Figure 5, PE1245-1, PE1234-1 and PE135-1, were then constructed from PE123456-1, where:

- (a) To construct the PE1245-1 system, $1 \times 2 \times 2$ unit cells of PE123456-1 were converted into a superlattice, the vertical ethylene chains were removed, and hydrogens were added to the phenyl rings, as shown in Figure 5(a);
- (b) To construct the PE1234-1 system, $1 \times 3 \times 3$ unit cells of PE123456-1 were converted into a superlattice, after which, nine ethylene bonds connecting phenyl rings, were removed, and replaced by hydrogen bonds, as is depicted in Figure 5(b);

- (c) To construct the PE135-1 system, $1 \times 3 \times 3$ unit cells of PE123456-1 were converted into a superlattice, after which, a phenyl ring and each of its six ethylene side chains were removed from the structure, and subsequently replaced with the sufficient amount of hydrogen atoms, to create a hexagonal pore within the structure, as shown in Figure 5(c).

The remaining twenty-four structures were similarly constructed, on the basis of these four original structures, by increasing the length between phenyl rings. This was achieved by increasing double bonds in the ethylene chains, in a step-wise manner, resulting in unit cells of different cell parameters, flexibilities and mechanical properties, until systems with seven double bonds between rings were constructed.

2.3.2. Setting up of the energy expression

The potential energies for the twenty-eight systems so constructed were set up using the PCFF force-field, as described in Section 2.3, with the difference that the non-bond terms were summed up using Ewald [20]. One must note that this force-field was chosen, since similar systems based on poly(phenylacetylene), flexyne, and re-flexyne networks have also used PCFF [12, 15, 14]. Note that, the decision to simulate the systems of interest using force-field based methods over quantum mechanical-based methods was carried out purposefully since the use of quantum mechanical-based simulations, while being more accurate, has drawbacks, such as the that it is much more computationally and time intensive. Thus, the use of such a method would not have permitted the simulation of a larger and broader variety of systems than could have been possible within the given time frame. Furthermore, given that the scope of the simulations is to calculate the structural and mechanical properties of these systems, and not properties, such as electrical or thermal conductivity, which would have necessitated information about the electronic states of the system, the use of such more computationally intensive simulations is unjustifiable.

2.3.3. Identification of stable conformations via energy minimisation and quench molecular dynamics

Following the setting up of the energy expression, energy minimisation in the form of geometry optimisation was carried out. This was done by allowing the atomic positions and lattice parameters to change, in order to obtain lower-energy conformations. The minimisation process involved the automation of three subsequent runs of increasing fineness in terms of extent of convergence, from medium to fine and then ultra-fine, with each step running for 1000 iterations, or until the convergence criteria were met, making sure to set the cell to be optimised. The Smart minimiser, which involves successive runs of the steepest descent, ABNR, and *quasi*-Newton methods, as implemented within the Forcite module in Materials Studio was used. In the final minimisation, with ultra-fine settings, the convergence criteria used were as in Section 2.3 (*i.e.* a maximum energy change of 2×10^{-5} kcal mol⁻¹ between minimisation steps, a maximum force of 1×10^{-3}

kcal mol⁻¹ Å⁻¹, and a maximum atom displacement of 1×10^{-5} Å) with the added requirement of a maximum stress of 1×10^{-3} GPa.

Furthermore, given that, unlike their poly(phenylacetylene) equivalents, the PE networks modelled here were expected to have more flexibility, which may have possibly resulted in more than one *quasi*-equally stable minimum energy conformations, additional simulations were performed using the technique of Quench Molecular Dynamics. As with other simulations carried out, these were performed using the Forcite module in Materials Studio. Quench Dynamics is known to be an effective tool which may be used to determine possible minima, and search for low-energy structures within a given conformational space. This technique involves two main tasks; molecular dynamics simulations to produce a trajectory from which different structures are chosen at pre-defined intervals for geometry optimisations. These dynamics simulations are typically carried out at high enough temperatures to ensure that the system may overcome energy barriers. Ideally, molecular dynamics simulations are performed on large enough systems or supercells in favour of smaller unit cells, since systems with larger numbers of atoms ensure the acceptable mirroring of the velocities within Maxwell-Boltzmann distributions. In this particular case, the simulation box was left as just one unit cell since the scope of the dynamics simulations was to perturb the structure enough so that the quenched structures would give a representative sample of stable conformations afforded by these systems, a process which was not too dependent on a well-equilibrated molecular dynamics simulation. In fact, all the structures which were extracted from the molecular dynamics simulation were subjected to energy minimisations, rather than used as extracted.

In this case, the molecular dynamics simulation was run as NPT, with a time step of 1.0 fs. The target temperature and pressure were set to 500K and 0.0 GPa, respectively. A total of 50,000 steps (total simulation time of 50 ps) were carried out, with quenching occurring at every 5000 steps. Temperature and pressure were controlled by using ‘Nosé’ thermostat [21] and ‘Berendsen’ barostat [22], respectively. With regards to the successive geometry optimisation simulations that were carried out, all settings as previously outlined in Section 2.2 were replicated, at ultra-fine quality in terms of convergence criteria. The Smart minimiser, as implemented in the Forcite module within Materials Studio was used. This process resulted in the identification of 11 structures, for each of the 28 initial structures, totalling 308 structures, which are shown in the results section, below.

2.4. Results and discussion: The structural properties of crystalline systems

All simulations were carried out successfully, and in all cases, through the molecular dynamics trajectory and the quenching performed, it was possible to obtain a total of 11×28 minimum energy conformers, each of which was minimised to the required energy convergence criteria.

A representative sample, of these minimum energy conformers, are shown in Figure 6, together with graphs (see Figure 7) showing data on the cell parameters, most notably showing the separation between layers against number of occurrences. These results bring out a number of important structural characteristics associated with these systems, as discussed below.

First and foremost, the images showing a $1 \times 2 \times 2$ unit cell, which permit a focus on the structural properties of the individual layers, suggest that the main findings reported in Section 2.3 also feature for the networks. In particular, to a first approximation, the systems minimise to a conformation which has the geometric characteristics of the macro-models they are meant to mimic, namely the wine-rack-like geometry [13, 14] for the PA1245- n systems, the polytriangles geometry [23] for the PA1234- n systems, and the hexagonal honeycombs [24] for the PA-135- n systems. This is clearly evident from Figure 8, which compares an example of these networks for $n=3$ with their respective PE systems and idealised macro-mechanical model. In the case of the fully substituted network, the PE optimised system, also features the expected characteristics.

A more detailed analysis of these structures, also highlights some other interesting features. For example, the chains in the PE systems appear not as straight as their respective PA counterparts, with the flexure featuring both in-plane and out-of-plane. Another interesting feature is that as a result of the manner of construction, the phenyl rings appear as chiral units, having rotational symmetry of order 6 in the case of PE123456- n , order 3 in the case of PE135- n , and order 2 in the case of PE1245- n . The out-of-plane flexure results in the systems having a higher separation between layers when compared to their PA counterparts. This added thickness is evident from the images of the projections of the networks in the xz -plane, and as discussed below, is likely to be an important factor in determining the manner by which these networks stack in 3D, allowing for distortions observed on the smaller systems involving the building blocks.

A look at the table which shows the cell parameters and the projections of the network in the x , y and z direction, highlights a very important distinction between the PE systems modelled here and their equivalents modelled elsewhere [14]. In said work, it was generally reported that the systems stack in a manner similar to what is observed in graphite-like stacking. Additionally, Grima and Evans [23], reported that the minimum energy separation between the different layers was found to be approximately 3.6 \AA , a distance which indicates the π - π interactions in between the different layers are being well represented. This distance, of 3.6 \AA is in fact very similar to the well-known value for graphite. In the present work,

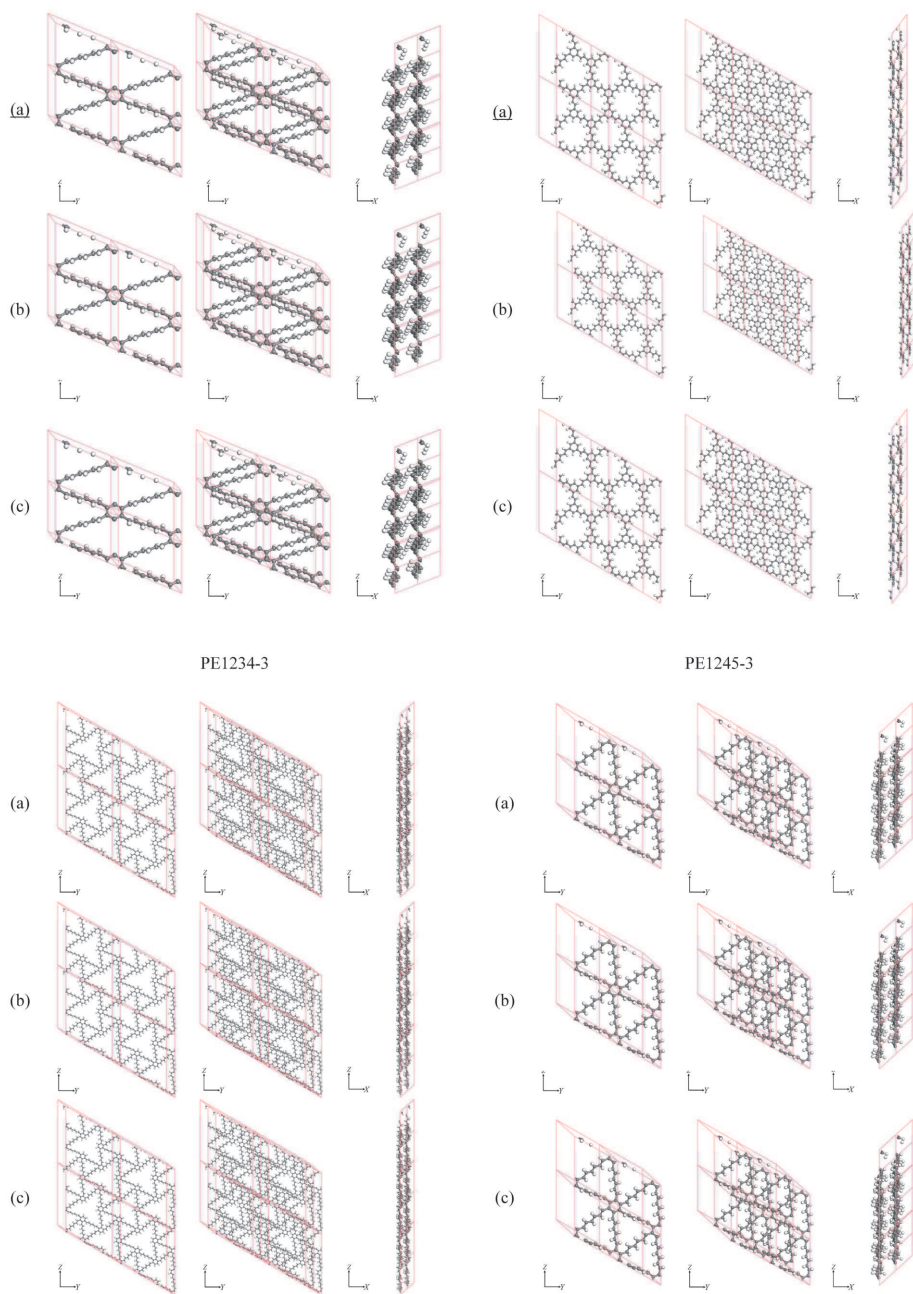


Figure 6. A representative sample of minimum energy conformers of the 4 modelled systems, namely PE123456-3, PE135-3, PE1234-3 and PE1245-3

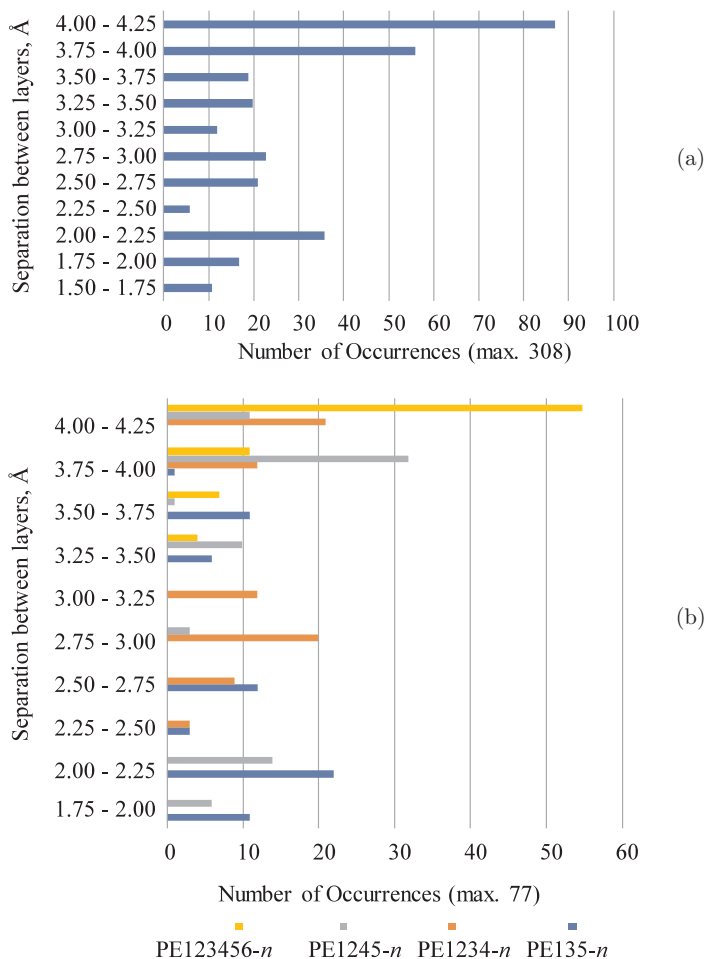


Figure 7. Data on the cell parameters, as seen by graphs of separation between layers in Å, against number of occurrences for the different systems modelled

the separation between layers varied over a much wider range, with the PE135- n and PE1234- n systems sometimes stacking at extremely short distances of < 2 Å, as shown in Figure 7, with the overall, most predominant separation being > 4 Å. This suggests, that despite having highly delocalised systems, the networks modelled in this study are not stacking in a manner which is conducive to optimal π - π stacking. This effect is very evident if one had to look at images showing $2 \times 2 \times 2$ (*i.e.* having more than one layer showing), rather than $1 \times 2 \times 2$, which clearly suggest that in this case the networks are not being aligned with a *quasi*-perfect stacking with their phenyl rings coinciding. Instead, the 11 structures, outputted by the quenching dynamics simulations all seem to adopt rather different stacking patterns with no general emergent trends.

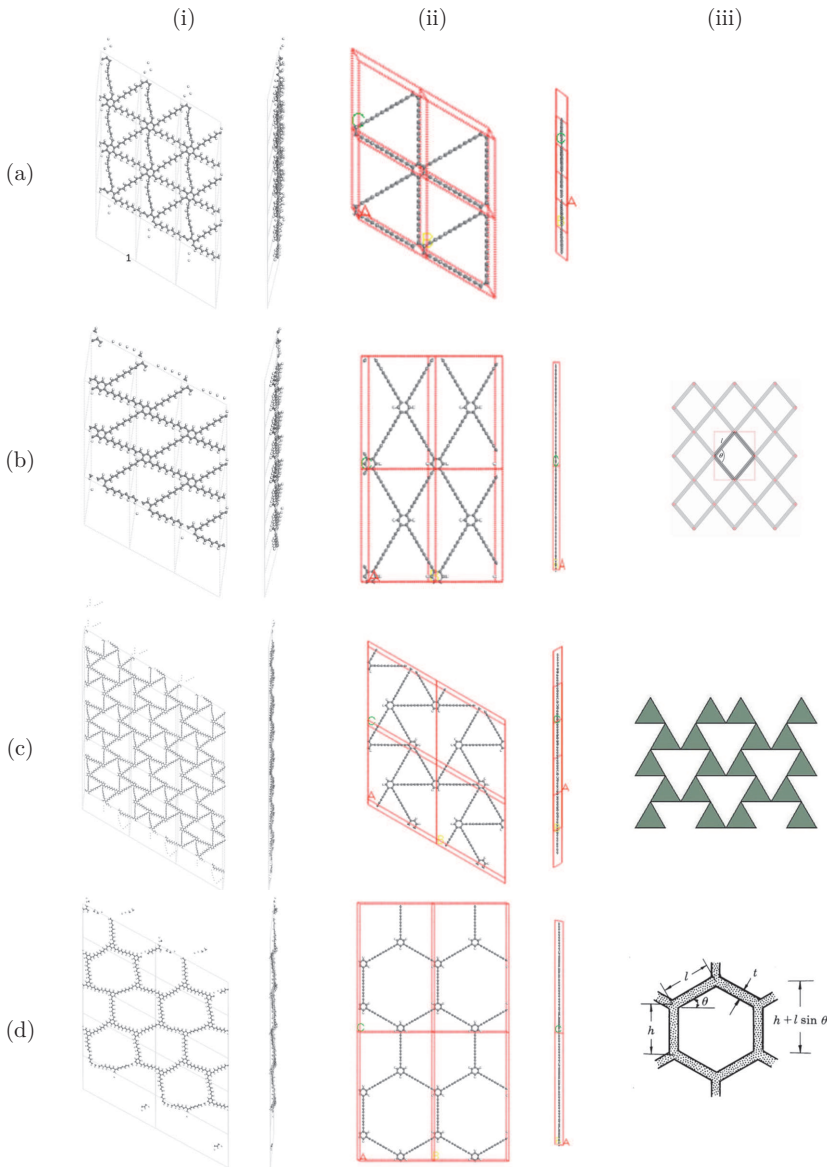


Figure 8. A comparison of the (a) PA123456-3; (b) PA1245-3; (c) PA1234-3; and (d) PA135-3 systems with their respective PE systems and idealised macro-mechanical models

In fact, any inferences that can be made are not universal. For example, in the case of the PE135-*n* systems, there seems to be a preferred, but not unique manner of stacking, where the corner of one honeycomb corresponds to the centre of the ones above it and below it, as seen in Figure 6. This effect, is likely to be the cause of the wide distribution of inter-layer separations, and is probably caused by the disturbance created through the lack of planarity of the networks, which reduce the stacking efficiency, from a purely geometric perspective.

This effect, merits substantial further investigation, which was not possible within the limited time-frame of the present work. For example, it would be important to assess whether this effect is dependent on the size of unit cell used, or on the force field or on the partial charges attributed to the different atoms. It must also be emphasized that the manner of stacking is primarily controlled through non-bond interactions, in this case van der Waals and Coulombic terms, and thus, the method of applying cut-offs could also play a crucial effect. More importantly, it may be envisaged, that this variability in stacking could also have some effect on the macroscopic properties, including their ability, when applicable, to exhibit NPR. In view of this, the next chapter will attempt to assess the Poisson's ratios, shear moduli, Young's moduli, and compressibilities that such systems are likely to exhibit, in an attempt to obtain a better picture of the possible properties of PE systems.

2.5. Section Summary

This section has shown that whilst it is possible to construct the nano-level equivalents of various motifs which are well-known for their auxetic characteristics through the PA networks, the resulting networks seem to be less 'regular' than their PA counterparts. In particular, it was shown that the manner of stacking is considerably more erratic than that adopted by the PA systems, leading to difficulty in isolating unique and representative minima. In view of this, it is being suggested that future work should look in more detail into the stacking ability of such networks, and the mechanical properties afforded by such systems. The latter aspect will be considered in the next section.

3. Simulation of the Mechanical Properties and Calculations of on- and off-axis properties

3.1. Introduction

It is possible to design materials in such a way to exhibit particular geometric and mechanical properties, in order to produce systems exhibiting anomalous properties, such as NPR, nonetheless, such systems may be extremely difficult to synthesise. Extensive and ongoing research has been carried out over the past several years, regarding the potential properties and applications of hyper-conjugated carbon networks

In the previous chapter, the interesting structural properties of the proposed poly(phenylethylene), or PE, alternatives to the more well-studied poly(phenylacetylene), or PA, systems were demonstrated, showing that whilst, to a first approximation, these two systems are very similar in plane, they have a very distinct manner of stacking in 3D. This chapter will focus on the mechanical properties that these systems may exhibit, with a particular focus on the potential of these systems to exhibit negative Poisson's ratios, either on-axis or off-axis. This analysis will be performed entirely through the use of simulations within

Materials Studio 7.0, the results of which will be compared to those obtained in other studies for the PA systems.

3.2. Methodology

Given that the minimum energy conformations of the systems to be studied had already been computed, the procedure used to assess the mechanical properties for each of the eleven structures obtained for each of the initial twenty-eight structures prepared, totalling three-hundred and eight, as a result of the Quenching Molecular Dynamics simulations, were subjected to the same mechanical properties simulations and on and off-axis properties calculations. The procedure to calculate the mechanical properties involved:

1. The actual simulations of the system at different levels of applied strain;
2. Calculations of on-axis mechanical properties;
3. Calculation of the in-plane off-axis properties.

More specifically, following the energy minimisation procedure, the mechanical properties of each of the twenty-eight structures were determined using the Mechanical Properties Task within the Forcite module in Materials Studio. The procedure was run using a Perl Script, to minimise human error, and most settings were kept default and at ultra-fine quality, except for the summation of non-bond terms which was set to Ewald [20]. The procedure used by Forcite, simulates the system under successive levels of applied strains, applied uniaxially or in shear, so as to generate the required stress-strain plots. The program has an automated method for calculating both the 6×6 on-axis stiffness matrix \mathbf{C} , which relates stresses to the applied strains, as below:

$$\begin{pmatrix} \sigma_x \\ \sigma_y \\ \sigma_z \\ \tau_{yz} \\ \tau_{zx} \\ \tau_{xy} \end{pmatrix} = \begin{pmatrix} c_{11} & c_{12} & c_{13} & c_{14} & c_{15} & c_{16} \\ c_{21} & c_{22} & c_{23} & c_{24} & c_{25} & c_{26} \\ c_{31} & c_{32} & c_{33} & c_{34} & c_{35} & c_{36} \\ c_{41} & c_{42} & c_{43} & c_{44} & c_{45} & c_{46} \\ c_{51} & c_{52} & c_{53} & c_{54} & c_{55} & c_{56} \\ c_{61} & c_{62} & c_{63} & c_{64} & c_{65} & c_{66} \end{pmatrix} \begin{pmatrix} \varepsilon_x \\ \varepsilon_y \\ \varepsilon_z \\ \varepsilon_{yz} \\ \varepsilon_{zx} \\ \varepsilon_{xy} \end{pmatrix} \quad (1)$$

Furthermore, the program also outputs the compliance matrix \mathbf{S} , which is the inverse of the stiffness matrix, *i.e.* $\mathbf{S} = \mathbf{C}^{-1}$, the on-axis Poisson's ratio and Young's moduli. Additionally, from the compliance matrix one may also calculate the on-axis shear moduli and linear compressibility, as outlined below:

Poisson's Ratio:

$$v_{yz} = \frac{-s_{32}}{s_{22}} \quad (2)$$

$$v_{zy} = \frac{-s_{23}}{s_{33}} \quad (3)$$

Shear Modulus:

$$G_{yz} = \frac{1}{s_{44}} \quad (4)$$

Young's modulus:

$$E_y = \frac{1}{s_{22}} \quad (5)$$

$$E_y = \frac{1}{s_{33}} \quad (6)$$

Linear Compressibility:

$$\begin{aligned} \beta &= s_{21} + s_{22} + s_{23} \\ \beta &= s_{31} + s_{32} + s_{33} \end{aligned} \quad (7)$$

Furthermore, the on-axis stiffness and compliance matrix may also be transformed, using appropriate transformations as outlined by Nye [25], to obtain the off-axis properties, using the mathematical software tool Maple 2018.2 (MapleSoft™, a division of Waterloo Maple Inc. 2019). The resulting plots, seen in Figures 9–16, depict the off-axis plots showing Poisson’s ratio, Young’s modulus, shear modulus and linear compressibilities obtained for each of the modelled PE structures, namely PE1234-*n*, PE1245-*n*, PE135-*n* and PE123456-*n* (Figures 9–12), followed by depictions of the Poisson’s ratio plots calculated for each of the 11 repeatable structures obtained (Figures 13–16) as a result of the Quench Dynamics simulations performed (see Section 2), for each of the 28 initial structures.

For ease of interpretation, the off-axis plots are colour-coded, with the auxetic regions being shown in red, and the non-auxetic regions being shown in blue. This was performed since colour-coded representation of the graphs makes it easier to extract the potentially important properties of the structures studied, since it permits direct, visual interpretation of the data. The results clearly show some very important trends. In particular, as seen in Figure 9 and Figure 13, almost all of the PE1234-*n* systems which are meant to mimic auxetic rotating triangles model, exhibit auxetic characteristics, which in most cases is exhibited for loading in any direction in the plane. This highlights the robustness of the rotating triangles mechanism, for generating NPR behaviour. Nevertheless, it is also equally evident, that the systems are highly anisotropic, this being in sharp contrast to what was exhibited in the polytriangles systems, which showed in-planar isotropic behaviour which tends to -1 for the systems with longer chains, as was demonstrated in [6].

Another network which is generally being predicted to exhibit NPR behaviour, is the PE1245-*n* system, as depicted by Figure 10 and Figure 14, which is meant to mimic the wine-rack structure. These systems, are being predicted to exhibit highly anisotropic NPR, which alternates between positive and negative, depending on the direction of stretching. Here it must be mentioned that the wine-rack model, even in its idealised form, is also known to be highly anisotropic [13], and exhibits NPR for stretching in the vicinity of the directions of the ligaments, but is conventional and exhibits high positive Poisson’s ratio values for stretching along the main lines of symmetry. This once again highlights the relationship between geometry and mechanical properties, and once again confirms that the wine-rack model has considerable potential for use as a blue-print for auxetic materials. This model, apart from auxeticity, is also known for another anomalous mechanical property, that of negative linear compressibility or NLC. This property is also present in the PE1245-*n* networks, as evident from

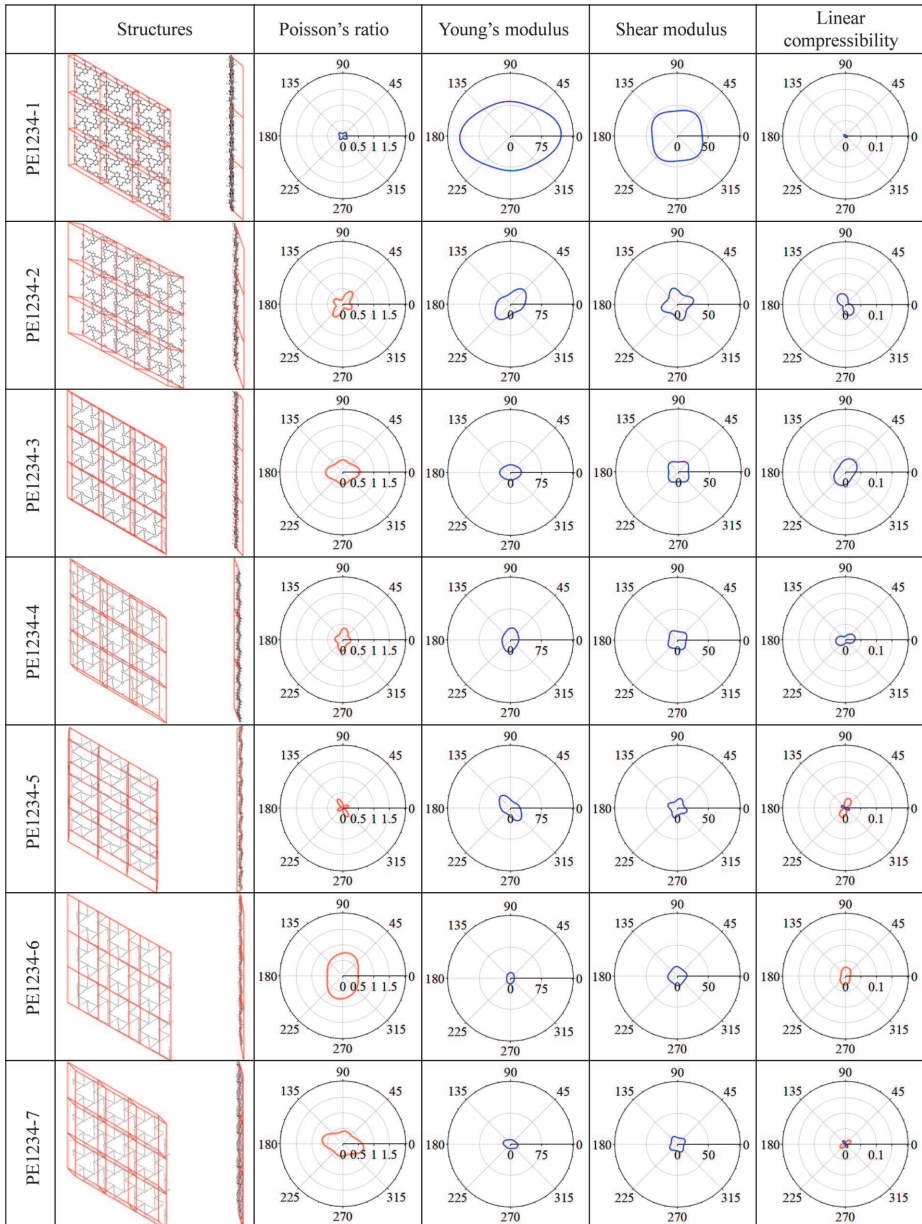


Figure 9. Off-axis plots of Poisson's ratio, Young's modulus, shear modulus and linear compressibilities obtained for each of the modelled PE structures of PE1234-*n*

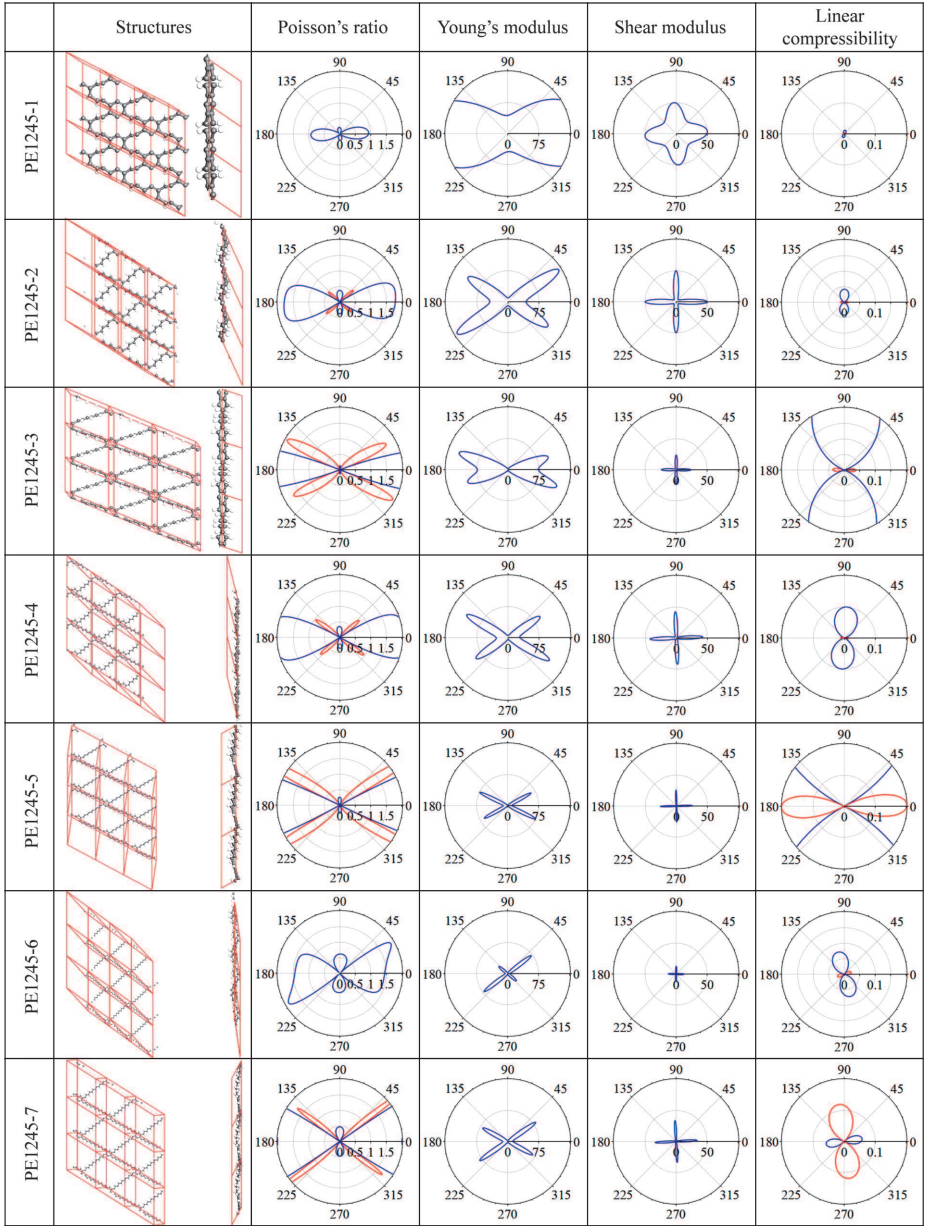


Figure 10. Off-axis plots of Poisson's ratio, Young's modulus, shear modulus and linear compressibilities obtained for each of the modelled PE structures of PE1245-*n*

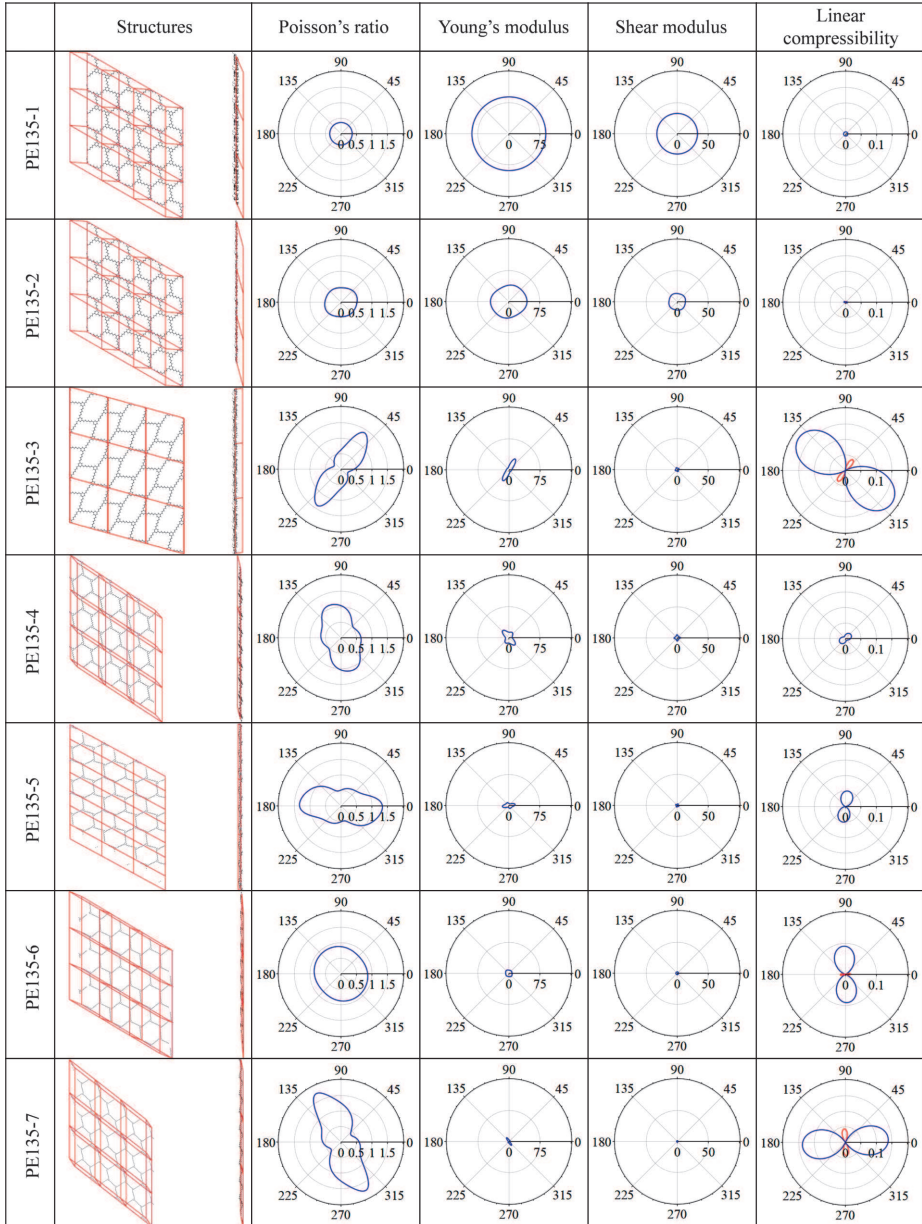


Figure 11. Off-axis plots of Poisson's ratio, Young's modulus, shear modulus and linear compressibilities obtained for each of the modelled PE structures of PE135-*n*

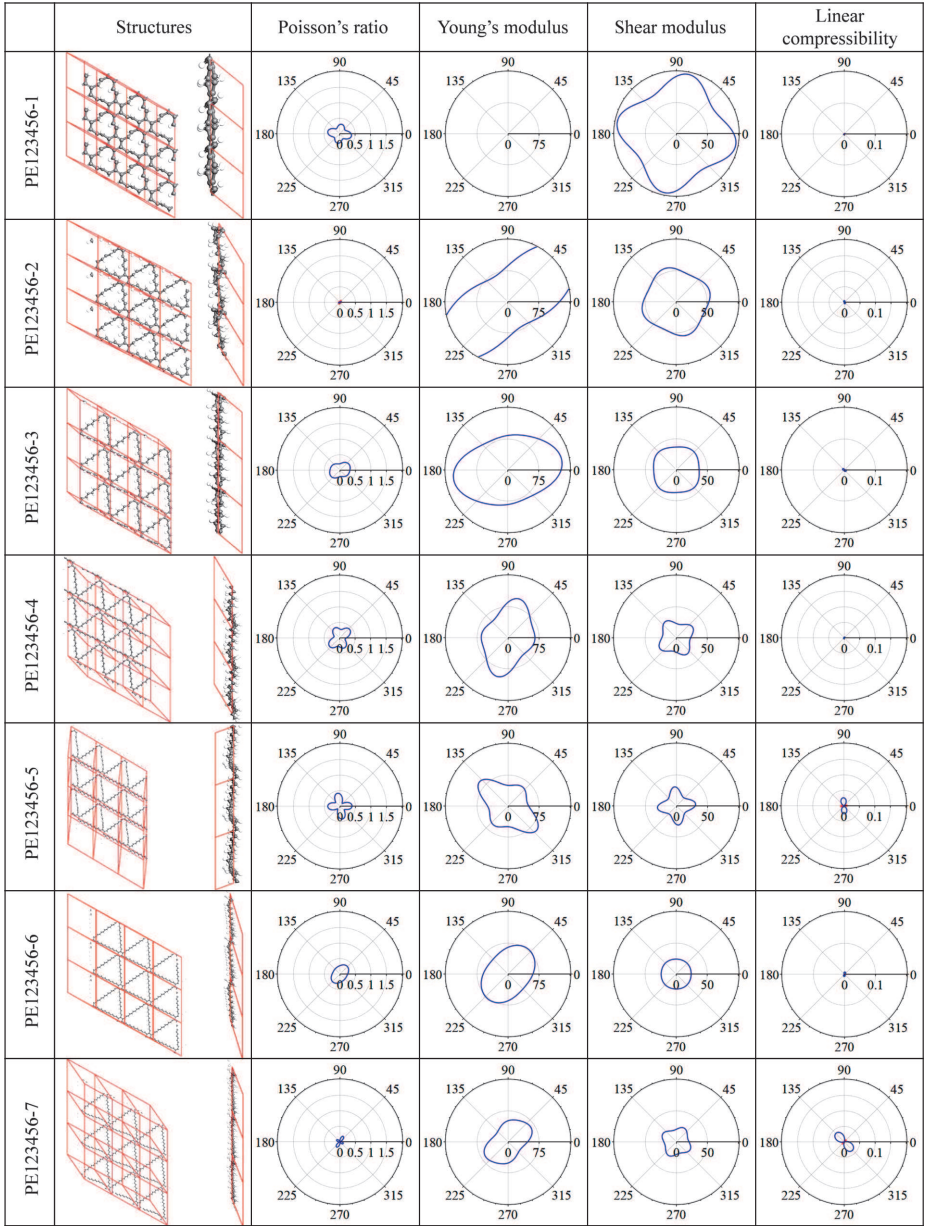


Figure 12. Off-axis plots of Poisson's ratio, Young's modulus, shear modulus and linear compressibilities obtained for each of the modelled PE structures of PE123456-*n*

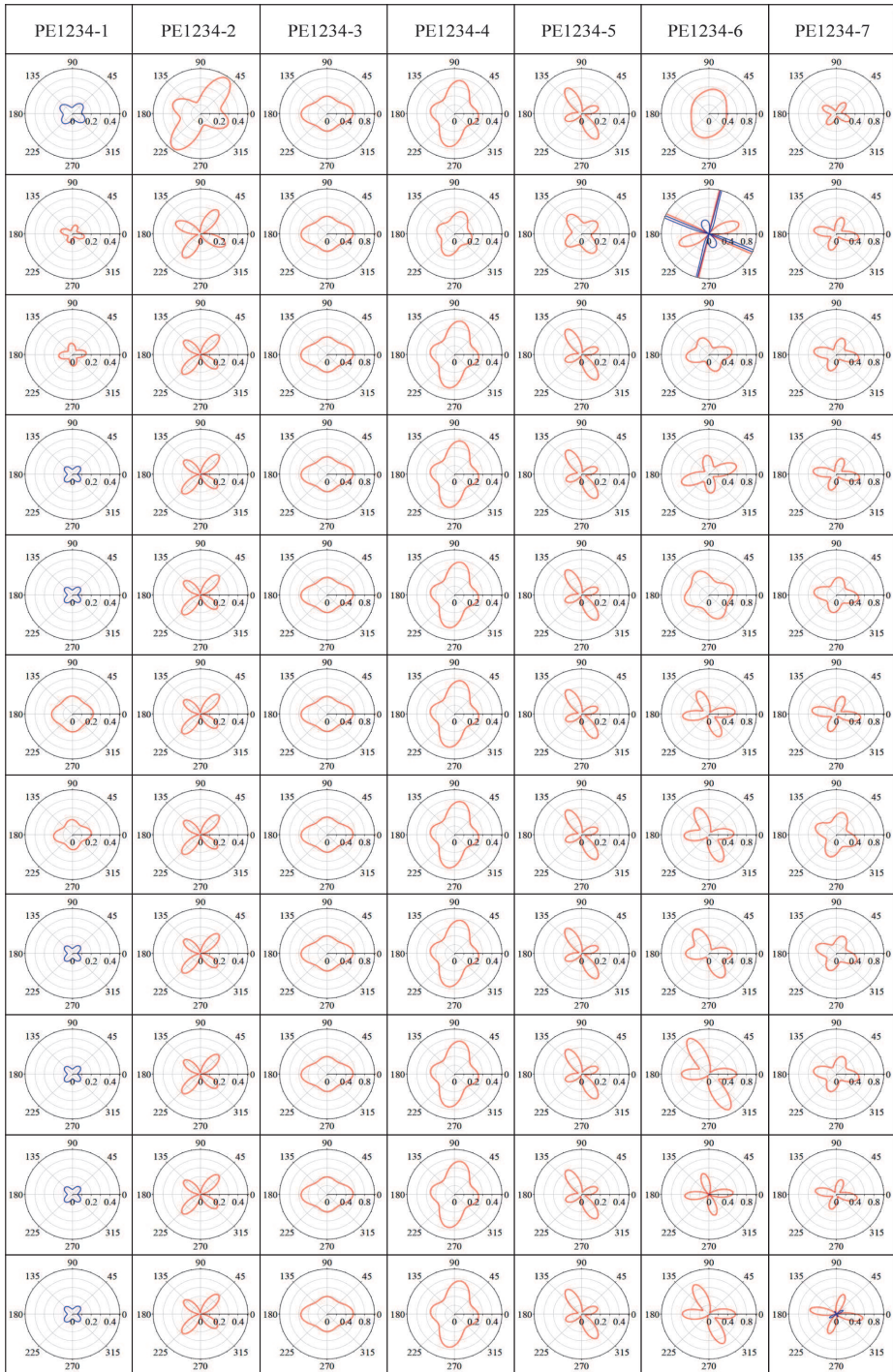


Figure 13. Off-axis Poisson's ratio plots calculated for each of the 11 repeatable structures obtained as a result of the Quench Dynamics simulations performed for PE1234-*n*

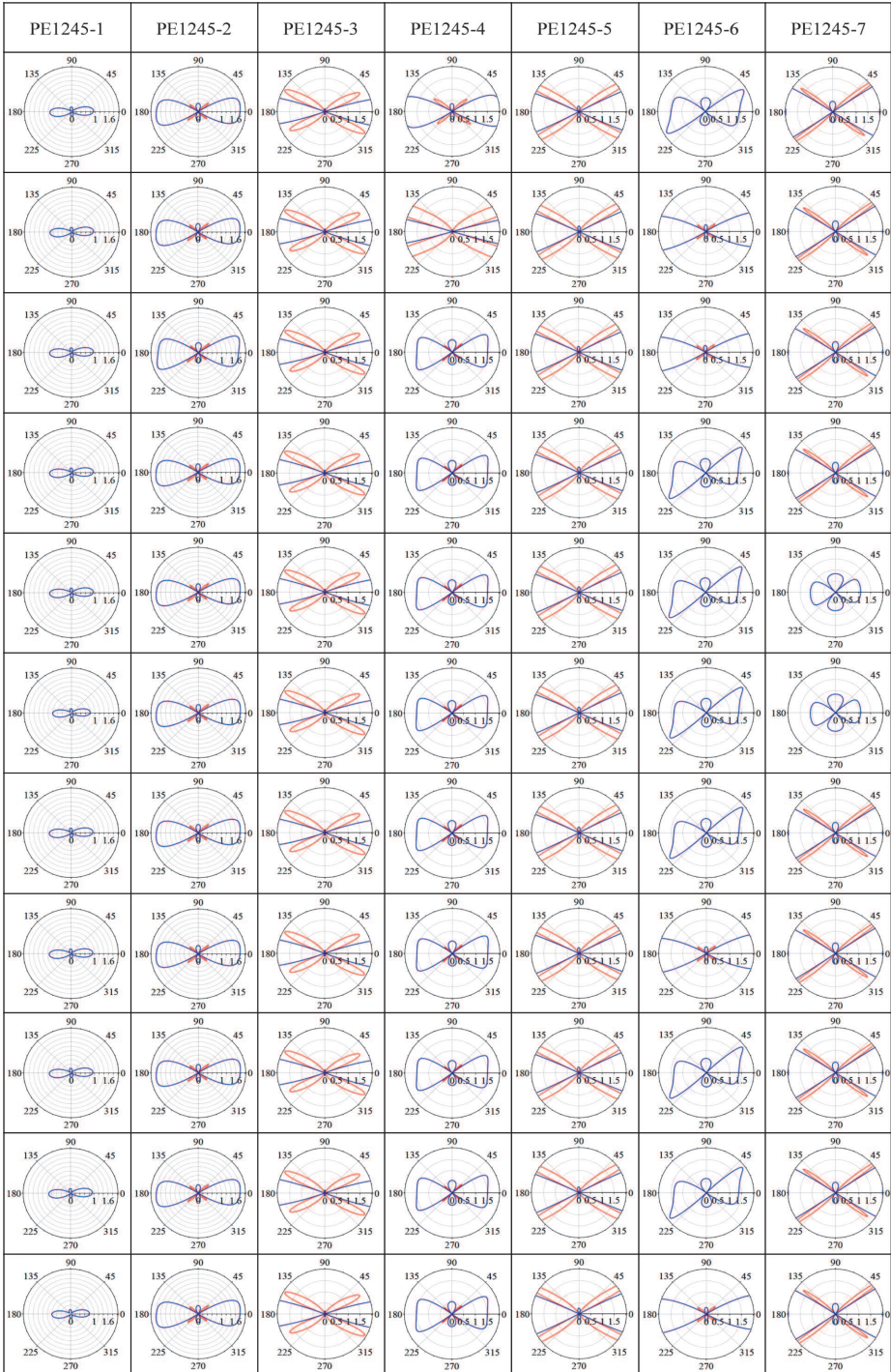


Figure 14. Off-axis Poisson's ratio plots calculated for each of the 11 repeatable structures obtained as a result of the Quench Dynamics simulations performed for PE1245-*n*

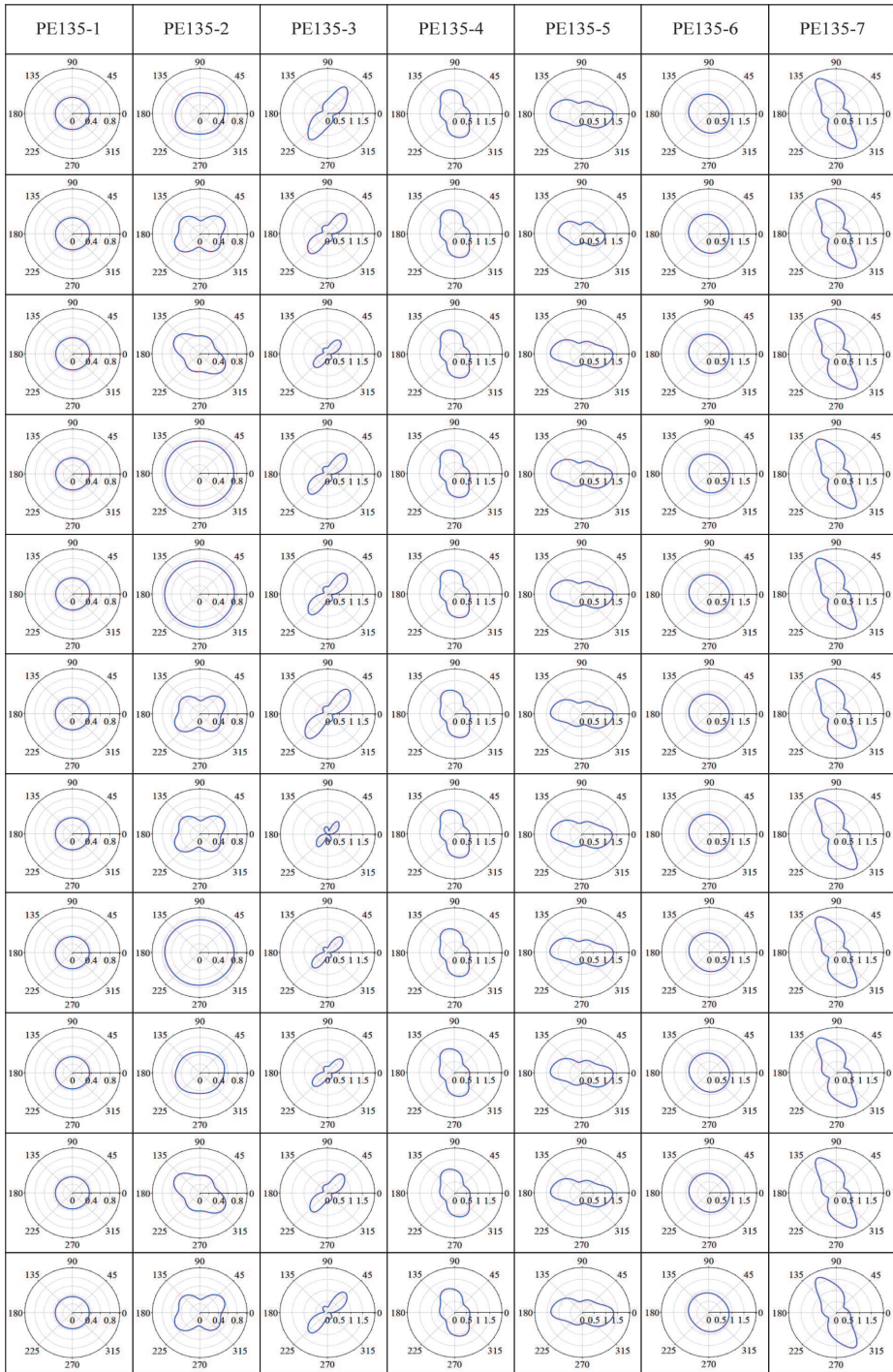


Figure 15. Off-axis Poisson's ratio plots calculated for each of the 11 repeatable structures obtained as a result of the Quench Dynamics simulations performed for PE135-*n*

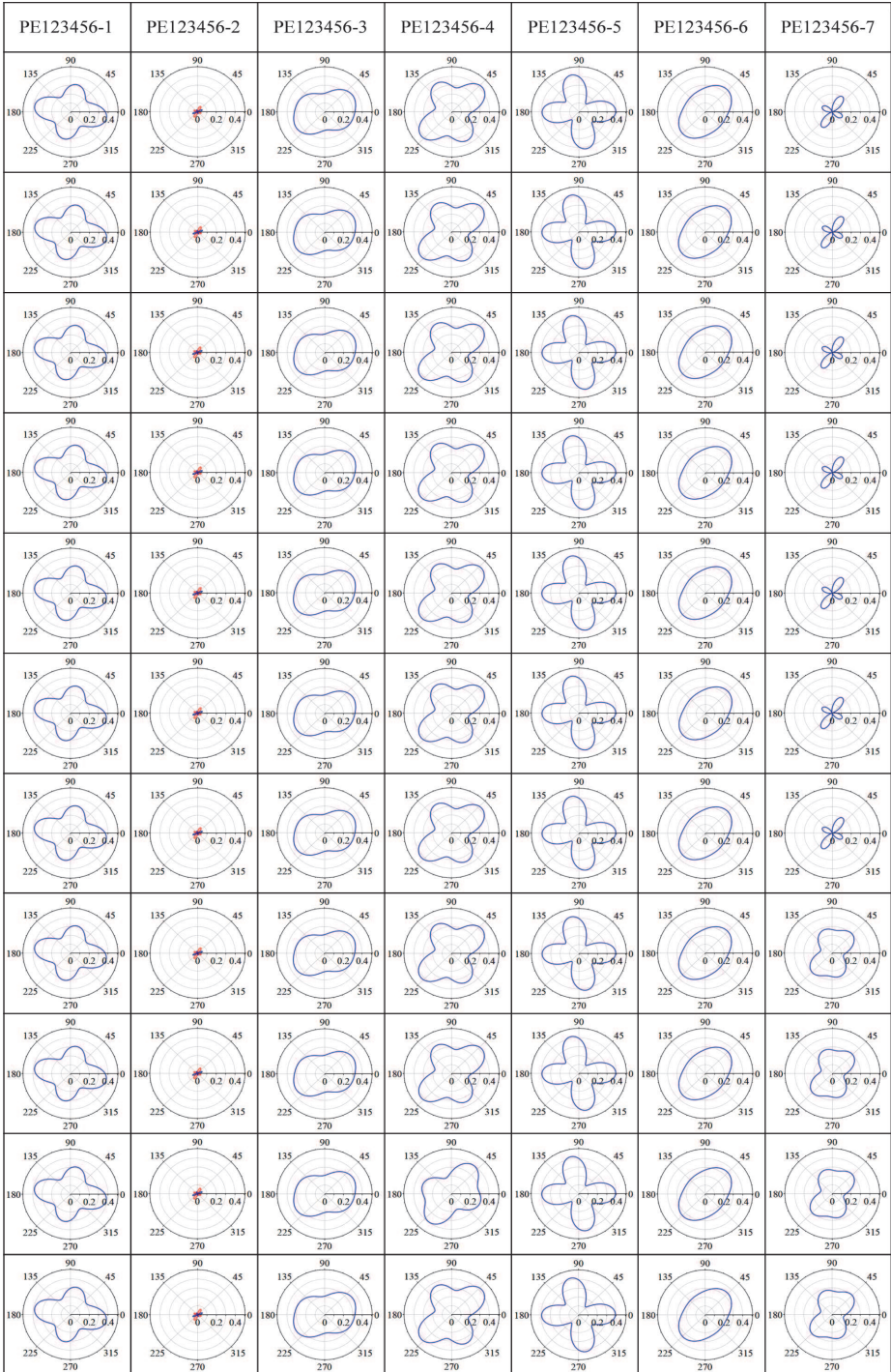


Figure 16. Off-axis Poisson's ratio plots calculated for each of the 11 repeatable structures obtained as a result of the Quench Dynamics simulations performed for PE123456-*n*

the results shown in Figure 10. These regions of NLC and NPR do not overlap, as expected, since NLC, through this mechanism requires the Poisson's ratio to be large and high.

With regards to the PE123456-*n*, or fully-substituted systems, anisotropy was observed, in all 7 of the different systems, with each of their respective 11 replicates (see Figure 16). Nonetheless, somewhat anomalously, a consistent, small NPR was observed in the case of structure PE123456-2, possibly due to a flattening mechanism occurring. It is therefore suggested that further research should be carried out on this structure in particular, to further assess the anomalous properties being identified in this preliminary study. Similarly, in the case of the PE135-*n*, or honeycomb-like systems, no negative properties were observed, though some anisotropy was noted in most structures, regardless of length of ethylene chain (see Figure 11, Figure 15).

Before concluding, it is important to emphasize that despite the trends and similarities observed above, the exact values of the mechanical properties have been predicted to vary (to various, non-equal extents) between one conformer and another of the same structure. Given that, in general, the 2D geometry of these different conformers were practically identical, this lack of repeatability, when present, is likely to be due to differences in the manner of stacking in 3D. Thus, this hypothesis needs to be further investigated, as if proved true, could provide researchers with a novel avenue on how to tailor-make the mechanical properties of these and related structures.

3.3. Section Summary

The present work showed that the simulations to calculate the mechanical properties of various poly(phenylethylene) crystalline networked polymers, were carried out successfully, and somewhat repeatably, as can be shown by the various Poisson's ratio plots resulting from the mechanical properties simulations carried out. Furthermore, it was shown that, to a first approximation, the Poisson's ratios for the respective structures generally agreed with the modelled predictions. As a result, several auxetic nanostructures have been identified, particularly in the PE1245-*n*, or wine rack-like system and PE1234-*n*, or polytriangles-like system. Nevertheless, as previously explained, the actual values of the Poisson's ratios obtained were observed to vary to various, non-equal extents between conformers of the same structure, which variation was primarily attributed to the unpredictable manner of stacking of these networks in 3D.

4. Conclusions and further work

This study has demonstrated that the construction of poly(phenylethylene) networks, was carried out successfully and through this work, novel cases of NPR and NLC were confirmed and identified, under specific conditions, along with the reporting of the dissimilar manner of 3D stacking of such systems, when compared to their well-studied counterparts – poly(phenylacetylene) networks – though to a somewhat less repeatable manner than expected.

More specifically, in Section 2, it was shown that notwithstanding the possibility of constructing the nano-level equivalents of various well-known poly(phenylacetylene) systems for their auxetic characteristics, the resulting poly(phenylethylene) networks were found to be less ‘regular’ than their counterparts. Furthermore, it was shown that the manner of 3D stacking was significantly more erratic than what is known to occur in the PA systems. This factor may have led to difficulties in the isolation of unique and representative minima.

As results from Section 3 suggest, the attempt to model the various poly(phenylethylene) crystalline networked polymers which were meant to mimic known macrostructures, was carried out successfully, and somewhat repeatably, as can be attested to by the various Poisson’s ratio plots resulting from the mechanical properties simulations carried out. Additionally, it was shown that, to a first approximation, the Poisson’s ratios for the respective structures generally agreed with the modelled predictions. In fact, several auxetic nanostructures have been identified, particularly in the PE1245-*n*, or wine rack-like system and PE1234-*n*, or polytriangles-like system. Nevertheless, as previously explained, the actual values of the Poisson’s ratios obtained were observed to vary to some extents between conformers of the same structure, where such a variation was primarily attributed to the unpredictable manner of stacking of these networks in the third dimension.

It is important to highlight possible avenues how this work can be examined in the future, as well as identify some of the strengths and limitations of the present work. First and foremost, the results presented in this dissertation, were all obtained from force-field based simulations, in lieu of quantum mechanical-based simulations, like density function theory (DFT) simulations, resulting in the omission of thermal and electrical properties calculations. Given the time constraints, and the preference of modelling a wider and more exhaustive variety of systems, less computationally intensive force field-based simulations were chosen, primarily due to the increased computational load imposed by DFT simulations. Nevertheless, unfortunately, the use of quantum mechanical simulations would be deemed necessary should one extend the analysis to also include the study of the effects of involving information about the electronic state of the system, such as, studies on conductivity. Given that the systems modelled here are hyper conjugated, it is envisaged that these systems are likely to benefit from enhanced conductivity properties, and hence it would be beneficial if in the future these systems will be studied using quantum mechanical simulations

Furthermore, the use of the PCFF force-field throughout the simulations carried out, whilst having significant advantages, namely the ability to easily inter-compare results derived from the systems modelled with results from systems from previous work carried out using the same force-field, poses a potential problem, with regards to force-field dependency. To ensure that the results obtained were indeed force-field independent, it is suggested that future work incorporates the use of other force-fields such as Dreiding and AIREBO.

Another important limitation of the current work was that due to the small size of the unit cell, the systems could have been made artificially too symmetric. For example, the use of just one layer within the unit cell, restricts the possible stacking patterns that such systems could be allowed to adopt. Thus, future work should look into the effect of unit cell size on the simulated structures and properties, with a view of ensuring that the systems modelled are indeed a true representation of what is expected to be present in these systems should they be synthesised.

Future work should also look at the effect of high temperatures and pressure on these systems, which effects can be best simulated using NPT molecular dynamics simulations. Unfortunately, for such simulations to be effective, it is required that the unit cell considered is much larger than the ones used for this study, so as to ensure the proper distribution of the particle velocities which would correspond to the thermodynamic temperature and sufficiently mirror the velocities within the Maxwell-Boltzmann distribution. In fact, as stated previously, one of the major limitations of this current work was that the unit cells were too small, and the dynamics runs were too short, a requirement which was necessitated by the fact that the simulations performed here had to be followed by a mechanical properties calculation, which is in itself resource-intensive. This can be exemplified as seen in the case of PE135-2, in which the same level of repeatability within the 11 different structures as seen in the other systems, was not observed. Nonetheless, for the scope of this work, the perturbation of the structures via quench dynamics, in order to ensure repeatability, which is not too dependent on well-equilibrated systems, was favoured over the thorough identification of all potential stable isomers that could be afforded.

As a result of the use of small unit cells used, in favour of larger super-cells, the analysis of large-scale effects was also omitted during this preliminary study, potentially disregarding any macroscale effects that could result from such modelled PE systems. Moreover, the use of dynamic simulations for non-dynamic systems was justified through the analysis of periodic 'snapshot' structures, and their respective mechanical and structural properties, which while not perfectly representative, allow for the general and essential inferences to be drawn. Furthermore, studies on the deformation mechanisms of the observed systems were not carried out, and hence it is being suggested that further work looks into the mechanical properties of systems under small strains, in order to determine what occurs at larger strains. This will allow for comparisons to be made with the deformation mechanisms of idealised macro-models, so as to draw similarities or differences between the models.

In conclusion, the main limitation of the present work is the inherent theoretical nature of the work, and notwithstanding the potential demonstrated by such PE systems, further work, especially regarding the aforementioned manner of 3D stacking is merited, to verify the hypothesised concepts, and extend on the current work.

References

- [1] Evans K E, Nkansah M A, Hutcherson I J and Rogers S C 1991 *Molecular Network Design*, **353**, **6340** 124 doi: <https://doi.org/10.1038/353124a0>
- [2] Evans K E, Nkansah M A and Hutchinson I J 1994 *Auxetic Foams: Modelling Negative Poisson's Ratios*, *Acta Metall. Mater.* doi: [https://doi.org/10.1016/0956-7151\(94\)90145-7](https://doi.org/10.1016/0956-7151(94)90145-7)
- [3] Evans K E, Alderson A and Christian F R 1995 *Auxetic Two-Dimensional Polymer Networks. An Example of Tailoring Geometry for Specific Mechanical Properties*, *J. Chem. Soc. Faraday Trans.* **91** (16) 2671 doi: <https://doi.org/10.1039/ft9959102671>
- [4] Grima J N and Evans K E 2000 *Auxetic Behavior from Rotating Squares*, **19**, **17** 1563 doi: <https://doi.org/10.1023/A:1006781224002>
- [5] Grima J N, Farrugia P-S, Gatt R and Attard D 2008 *On the Auxetic Properties of Rotating Rhombi and Parallelograms: A Preliminary Investigation*, *Phys. Status Solidi Basic Res.* **245** (3) doi: <https://doi.org/10.1002/pssb.200777705>
- [6] Grima J N, Oliveri L, Attard D, Ellul B, Gatt R, Cicala G and Recca G 2010 *Hexagonal Honeycombs with Zero Poisson's Ratios and Enhanced Stiffness*, *Adv. Eng. Mater.* **12** (9) doi: <https://doi.org/10.1002/adem.201000140>
- [7] Grima J N, Chetcuti E, Manicaro E, Attard D, Camilleri M, Gatt R and Evans K E 2012 *On the Auxetic Properties of Generic Rotating Rigid Triangles*, **468**, **2139** 810 doi: <https://doi.org/10.1098/rspa.2011.0273>
- [8] Grima J N, Zerafa C and Brincat J-P 2014 *Development of Novel Poly(Phenylacetylene) Network Polymers and Their Mechanical Behaviour*, *Phys. Status Solidi Basic Res.* **251** (2) doi: <https://doi.org/10.1002/pssb.201384254>
- [9] Grima J N, Degabriele E P and Attard D 2016 *Nano Networks Exhibiting Negative Linear Compressibility*, *Phys. Status Solidi Basic Res.* **253** (7) doi: <https://doi.org/10.1002/pssb.201600276>
- [10] Grima J N and Zerafa C 2013 *On the Effect of Solvent Molecules on the Structure and Mechanical Properties of Organic Poly(phenylacetylene) Auxetic Re-Entrant Network Polymers*, **250**, **10** doi: <https://doi.org/10.1002/pssb.201384245>
- [11] Trapani L, Gatt R, Mizzi L and Grima J N 2015 *Mechanical Properties of 2D Flexyne and Reflexyne Poly(phenylacetylene) Networks: A Comparative Computer Studies with Various Force-Fields*, *TASK Quart.* **19** (3) 237
- [12] Grima-Cornish J N, Grima J N and Evans K E 2017 *On the Structural and Mechanical Properties of Poly(Phenylacetylene) Truss-Like Hexagonal Hierarchical Nanonetworks*, *Phys. status solidi* **254** (12) 1700190 doi: <https://doi.org/10.1002/pssb.201700190>
- [13] Caruana-Gauci R, Degabriele E P, Attard D and Grima J N 2018 *Auxetic Metamaterials Inspired from Wine-Racks*, *J. Mater. Sci.* **53** (7) 5079 doi: <https://doi.org/10.1007/s10853-017-1875-y>
- [14] Degabriele E P, Attard D, Grima-Cornish J N, Caruana-Gauci R, Gatt R, Evans K E and Grima J N 2019 *On the Compressibility Properties of the Wine-Rack-Like Carbon Allotropes and Related Poly(Phenylacetylene) Systems*, *Phys. status solidi* **256** (1) 1800572 doi: <https://doi.org/10.1002/pssb.201800572>
- [15] Degabriele E P, Grima-Cornish J N, Attard D, Caruana-Gauci R, Gatt R, Evans K E and Grima J N 2017 *On the Mechanical Properties of Graphyne, Graphdiyne, and Other Poly(Phenylacetylene) Networks*, *Phys. status solidi* **254** (12) 1700380 doi: <https://doi.org/10.1002/pssb.201700380>
- [16] Hwang M J, Stockfisch T P and Hagler a T 1994 *Derivation of Class-Ii Force-Fields 2. Derivation and Characterization of a Class-Ii Force-Field, Cff93, for the Alkyl Functional-Group and Alkane Molecules*, *J. Am. Chem. Soc.* **116** (6) 2515 doi: <https://doi.org/10.1021/ja00085a036>
- [17] Maple J R, Hwang M-J, Stockfisch T P, Dinur U, Waldman M, Ewig C S and Hagler A T 1994 *Derivation of Class II Force Fields. I. Methodology and Quantum Force Field for*

- the Alkyl Functional Group and Alkane Molecules, J. Comput. Chem.* **15** (2) 162
doi: <https://doi.org/10.1002/jcc.540150207>
- [18] Rappe A K and Goddard W A 1991 *Charge Equilibration for Molecular Dynamics Simulations, J. Phys. Chem.* **95** (8) 3358 doi: <https://doi.org/10.1021/j100161a070>
- [19] Grima J N, Jackson R, Alderson A and Evans K E 2000 *Do Zeolites Have Negative Poisson's Ratios?*, *Adv. Mater.* **12** (24) 1912 doi: [https://doi.org/10.1002/1521-4095\(200012\)12:24<1912::AID-ADMA1912>3.0.CO;2-7](https://doi.org/10.1002/1521-4095(200012)12:24<1912::AID-ADMA1912>3.0.CO;2-7)
- [20] Ewald P P 1921 *Die Berechnung Optischer Und Elektrostatischer Gitterpotentiale*, *369* 253 doi: <https://doi.org/10.1002/andp.19213690304>
- [21] Nosé S 1991 *Constant Temperature Molecular Dynamics Methods*, 103 1
- [22] Berendsen H J C, Postma J P M, Van Gunsteren W F, Dinola A and Haak J R 1984 *Molecular Dynamics with Coupling to an External Bath, J. Chem. Phys.* **81** 3684
doi: <https://doi.org/10.1063/1.448118>
- [23] Grima J N and Evans K E 2006 *Auxetic Behavior from Rotating Triangles*, *41*, **10** 3193
doi: <https://doi.org/10.1007/s10853-006-6339-8>
- [24] Masters I G and Evans K E 1996 *Models for the Elastic Deformation of Honeycombs*, *35*, **4** 403 doi: [https://doi.org/10.1016/S0263-8223\(96\)00054-2](https://doi.org/10.1016/S0263-8223(96)00054-2)
- [25] Nye J F 1957 *Physical Properties of Crystals: Their Representations by Tensors and Matrices*

